

Soft Maximin Aggregation of Heterogeneous Array Data

Adam Lund, Søren Wengel Mogensen, and Niels Richard Hansen *

December 14, 2024

Abstract

The extraction of a common signal across many recordings is difficult when each recording – in addition to the signal – contains large, unique variation components. This is observed for voltage sensitive dye imaging (VDSI), an imaging technique used to measure neuronal activity, for which the resulting 3D array data have a highly heterogeneous noise structure. Maximin aggregation (magging) has previously been proposed as a robust estimation method in the presence of heterogeneous noise. We propose soft maximin aggregation as a general methodology for estimating a common signal from heterogeneous data. The soft maximin loss is introduced as an aggregation of explained variances, and the estimator is obtained by minimizing the penalized soft maximin loss. By establishing properties of the general soft maximin aggregation loss we are able to show convergence of a proximal gradient based algorithm when applied to the estimation problem. Using this we obtain a time and memory efficient algorithm for data with tensor-array structure. The implementation is provided in the R package *SMMA* available from CRAN. We demonstrate that soft maximin aggregation performs well on a VSDI data set with 275 recordings, for which magging does not work.

VSDI data, optimization, sparse estimation, array-tensor structure, proximal gradient algorithm

1 Introduction

We consider the problem of extracting a common signal from heterogeneous groups of data. This is exemplified by spatio-temporal array data on neuronal activity recorded repeatedly over time for 13 ferrets, the objective being to extract a common neuronal response to a visual stimulus.

We will regard each 3D neuronal activity recording as a sample from a linear model with a mean component expressed in a basis expansion. If the mean

*University of Copenhagen, Department of Mathematical Sciences, Universitetsparken 5, 2100 Copenhagen Ø, Denmark, e-mail: adam.lund@math.ku.dk (A. Lund).

components across all recordings are identical, the common mean component can be interpreted as the common signal and extracted via least squares estimation of the basis coefficient, say. However, the recordings are heterogeneous in the sense that the mean component cannot be regarded as fixed. Heterogeneity can, for instance, arise across recordings for a single animal due to slightly varying experimental conditions or to fatigue, and spatial heterogeneity is expected across animals due to differences in the cytoarchitecture. Various preprocessing techniques such as registration are used to alleviate heterogeneity, but preprocessing may only be partially successful, and human assessment for e.g. exclusion of outliers was needed in Roland et al. (2006).

Explicit modeling of heterogeneity is possible and studied in the field of functional data analysis, Scheipl et al. (2015); Staicu et al. (2010); Wang et al. (2016), but we will not pursue this more sophisticated modeling framework. Though heterogeneity may represent structured variation, it may have many different known as well as unknown origins, and our focus is on fast, robust estimation of a common signal.

Meinshausen and Bühlmann (2015) proposed the maximin method as a way to aggregate heterogeneous data within the framework of linear models. Their population quantity called the maximin effect is the common signal, and they proposed families of estimators, see (9) in Meinshausen and Bühlmann (2015). These maximin estimators are, however, difficult to compute. Though they are given as solutions to convex minimization problems, the objective functions are nondifferentiable as well as nonseparable.

An approach to circumvent the computational difficulties was proposed in another paper by Bühlmann and Meinshausen (2016). Using a theoretical representation of the maximin effect combined with the plug-in principle, they proposed magging (maximin aggregation) as an estimator of the maximin effect. Though magging is computationally applicable to the neuronal activity recordings, we will demonstrate that it does not successfully extract a common signal.

We propose the soft maximin estimator, which may be viewed as a computationally well behaved approximation to maximin estimation and an alternative to magging. More importantly, it offers an entire range of estimators of independent interest interpolating magging and mean aggregation. By aggregating explained variances (or more generally convex group loss functions) using a type of soft minimum we obtain the estimator as a solution to a minimization problem with a differentiable loss. We refer to this loss function as the soft maximin loss and the estimator solves the soft maximin problem. Furthermore, to obtain a sparse solution across groups we consider an ℓ_1 -penalized version of this problem.

For array data, such as the 3D neuronal activity recordings, we have previously demonstrated the efficiency of proximal gradient algorithms for sparse smoothing using tensor product bases, Lund et al. (2017). In this paper we establish that the soft maximin loss is strongly convex under a full rank assumption on the design matrices (strongly convex group loss functions). We also show that the soft maximin loss has a Lipschitz continuous gradient when the

design is identical across groups. Using this it's possible to show convergence of a proximal gradient based algorithm when applied to the penalized soft maximin problem. As in Lund et al. (2017) we can then exploit the array-tensor structure of the data to obtain a time and space efficient solution algorithm for this type of problem. An implementation is provided in the R package SMMA available from CRAN, Lund (2017).

The paper is organized as follows: The model setup and the soft maximin estimator is introduced in Section 2 and a small 1D example with simulated data is presented. In Section 3 we establish properties of the soft maximin loss and the convergence of the NPG algorithm within this setup. We also discuss how to exploit the array-tensor structure with this algorithm, and illustrate our method on a 3D signal extraction example. Section 4 presents the application to the neuronal activity data, and in Section 5 we discuss soft maximin estimation and how it relates to alternative methods.

2 Soft maximin problem

We consider the linear model

$$Y_{g,i} = X_{g,i}^\top B_g + \varepsilon_{g,i}, \quad g = 1, \dots, G, \quad i = 1, \dots, n_g \quad (1)$$

with G groups, and with $X_{g,i}$ as well as B_g p -dimensional vectors. Depending on the context, $X_{g,i}$ and B_g may be regarded as fixed or they may be regarded as random as in Meinshausen and Bühlmann (2015). In any case, the errors, $\varepsilon_{g,i}$, are assumed uncorrelated with mean zero given $(X_{g,i}, B_g)_{g,i}$. Within this linear modeling framework, heterogeneity across the groups is captured by the variation in the B_g -coefficients.

We let $Y_g = (Y_{g,1}, \dots, Y_{g,n_g})^\top$ denote the group-specific response vector of length n_g , $X_g = (X_{g,1}, \dots, X_{g,n_g})^\top$ denotes the corresponding $n_g \times p$ design matrix, and $\varepsilon_g = (\varepsilon_{g,1}, \dots, \varepsilon_{g,n_g})^\top$ denotes the vector of error terms. The linear model for the g th group is then

$$Y_g = X_g B_g + \varepsilon_g. \quad (2)$$

A *common signal* in this framework is represented by a single $\beta \in \mathbb{R}^p$ such that $X_g \beta$ is a good approximation of $X_g B_g$ across all G groups. Following Meinshausen and Bühlmann (2015), the empirical explained variance of $\beta \in \mathbb{R}^p$ for group g is defined as

$$\hat{V}_g(\beta) := \frac{1}{n_g} (2\beta^\top X_g^\top y_g - \beta^\top X_g^\top X_g \beta). \quad (3)$$

Clearly, $\hat{\beta}_g = \arg \max_\beta \hat{V}_g(\beta)$ is the OLS estimator within group g .

The maximin effects estimator proposed in Meinshausen and Bühlmann (2015) is obtained by maximizing the minimum of (3) across groups. The

resulting optimization problem is difficult given the nondifferentiability and nonseparability of the min function.

We propose the soft maximin estimator obtained by maximizing a soft minimum of (3) across groups. For $x \in \mathbb{R}^G$ and $\zeta \neq 0$ consider the scaled log-sum exponential function

$$\text{lse}_\zeta(x) := \frac{\log(\sum_g e^{\zeta x_g})}{\zeta}.$$

As argued below lse_ζ behaves as a soft maximum (minimum) for large positive (negative) values of ζ . Letting $\hat{V}(\beta) = (\hat{V}_1(\beta), \dots, \hat{V}_G(\beta))^\top$ denote the vector of explained variances, we shall refer to

$$l_\zeta(\beta) := \text{lse}_\zeta(-\hat{V}(\beta))$$

as the soft maximin loss function. Noting that $\text{lse}_{-\zeta}(x) = -\text{lse}_\zeta(-x)$, the soft maximin estimator is then defined for $\zeta > 0$ as

$$\beta_{smm} := \arg \max_{\beta \in \mathbb{R}^p} \text{lse}_{-\zeta}(\hat{V}(\beta)) = \arg \min_{\beta \in \mathbb{R}^p} l_\zeta(\beta). \quad (4)$$

Note that l'Hôpital's rule gives $\text{lse}_{-\zeta}(x) \rightarrow \min\{x\}$ for $\zeta \rightarrow \infty$. For large $\zeta > 0$ we can therefore view the soft maximin estimator (4) as an approximation to the maximin estimator proposed in Meinshausen and Bühlmann (2015). Note also that soft maximin estimation puts less weight on the groups with the smallest explained variance than maximin estimation. Especially, using that

$$\frac{\log(\frac{1}{G} \sum_g e^{\zeta x_g})}{\zeta} \rightarrow \frac{1}{G} \sum_g x_g$$

for $\zeta \rightarrow 0$, we see that $\text{lse}_\zeta(x) \sim \frac{1}{G} \sum_g x_g + \frac{\log(G)}{\zeta}$ for small ζ . Thus the soft maximin loss can be seen as an interpolation between mean aggregation and max aggregation of minus the explained variances.

2.1 Smoothing

As a main example of soft maximin aggregation we will consider smoothing of signals over a multivariate domain from G groups. Thus

$$Y_{g,i} = f_g(z_{g,i}) + \varepsilon_{g,i}, \quad z_{g,i} \in \mathbb{R}^d, \quad i = 1, \dots, n_g, \quad (5)$$

with f_g a group specific smooth function. If we represent f_g using a basis expansion as

$$f_g(z) = \sum_{m=1}^p \Theta_{g,m} \varphi_m(z), \quad (6)$$

for $\varphi_1, \dots, \varphi_p$ a set of basis functions, we can collect the basis function evaluations into the $n_g \times p$ matrix $\Phi_g = (\varphi_m(z_{g,i}))_{i,m}$, in which case model (5) is given as the linear model (2) with $X_g = \Phi_g$ and $B_g = (\Theta_{g,1}, \dots, \Theta_{g,p})^\top$.

2.2 1-dimensional signal extraction

To illustrate how soft maximin estimation works, we reproduce and extend the numerical example from Bühlmann and Meinshausen (2016). We simulate signals with three components: i) a common signal of interest $f(x) = \cos(10(2\pi)x) + 1.5 \sin(5(2\pi)x)$ superimposed with ii) periodic signals with randomly varying frequency and phase and iii) additive white noise. In particular, we simulate $G = 50$ signals where for each $g \in \{1, \dots, 50\}$

$$Y_{g,i} = f(x_i) + 50 \sum_{j \in J_g} \varphi_j(x_i + p_g) + \varepsilon_{g,i}, \quad i = 1, \dots, 2001.$$

Here J_g is a set of 7 integers sampled uniformly from $\{1, \dots, 101\}$, φ_j is the j th Fourier basis function, $p_g \sim \text{unif}(-\pi, \pi)$, and $\varepsilon_{g,i} \sim \mathcal{N}(0, 10)$. We simulate observations for each $x_i = 0, 1, \dots, 2000$.

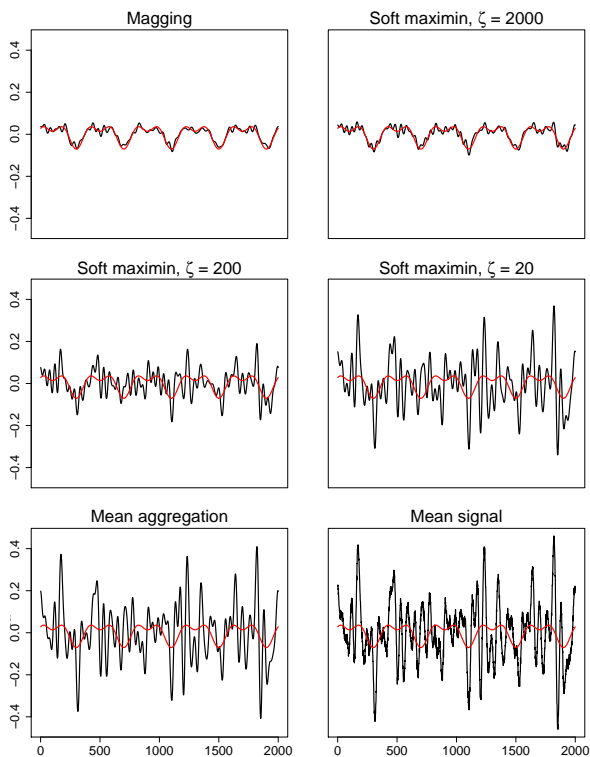


Figure 1: True signal in red. From top left we have the magging estimate, the soft maximin estimates for $\zeta = 2000, 200$, and 20 , the mean aggregated estimate and the mean signal, which is simply the average across groups. The MSE for the magging estimate is 1.301×10^{-4} and 1.953×10^{-4} for the soft maximin estimate ($\zeta = 2000$).

With Φ containing the 101 first Fourier basis functions evaluated at $x_i = 0, 1, \dots, 2000$ we solved an ℓ_1 penalized soft maximin problem (see (7) below) for a sequence of penalty parameters and for $\zeta = 20, 200$, and 2000.

In addition, we aggregated the groupwise OLS estimates, $\hat{\beta}_1, \dots, \hat{\beta}_{50}$, using magging as proposed in Bühlmann and Meinshausen (2016) as well as by mean aggregation. The mean signal across groups was also computed.

Figure 1 shows the results of the different estimation procedures. Both the magging estimate and the soft maximin estimate for $\zeta = 2000$ extracted the true common signal quite well, while the mean aggregated estimate resembled the mean signal showing little similarity to the common signal. We note that for larger ζ soft maximin behaved similarly to magging, while for smaller ζ soft maximin resembled mean aggregation as expected.

3 Penalized soft maximin aggregation

Here we formulate a general penalized soft maximin *aggregation* problem. Instead of $-\hat{V}$ defined in (3) we consider a general set of group loss functions $h := (h_1, \dots, h_G)$ and the soft maximin aggregation loss $s_\zeta : \mathbb{R}^p \rightarrow \mathbb{R}$, given by

$$s_\zeta(\beta) := \text{lse}_\zeta \circ h(\beta) = \frac{\log(\sum_{g=1}^G e^{\zeta h_g(\beta)})}{\zeta}, \quad \zeta > 0.$$

We are then interested in obtaining the penalized soft maximin aggregation estimator defined as the solution to the problem

$$\min_{\beta \in \mathbb{R}^p} s_\zeta(\beta) + \lambda J(\beta), \quad \zeta > 0, \quad (7)$$

where J is a proper convex function and $\lambda \geq 0$ is the penalty parameter. When $h = -\hat{V}$ as in section 2, we refer to $s_\zeta = l_\zeta$ as the soft maximin loss and to (7) as the penalized soft maximin problem. Thus the term *aggregation* is used to emphasize that we are considering general group loss functions h_1, \dots, h_G .

Solving (7) in a large scale setting requires an efficient optimization algorithm for non-differentiable problems. We note that when $h = -\hat{V}$, in contrast to the hard maximin problem from Meinshausen and Bühlmann (2015), (7) is a convex nondifferentiable and also separable problem (see Tseng and Yun (2009)) implying that the coordinate descent algorithm is a viable for the problem (7). Here however, since we are particularly interested in solving (7) for data with array-tensor structure we are going to consider modified versions of the proximal gradient algorithm. As demonstrated in Lund et al. (2017) this algorithm is very well suited to handle this particular setup and can outperform the coordinate descent algorithm.

The proximal gradient algorithm fundamentally works by iteratively applying the proximal operator

$$\text{prox}_{\delta J}(\beta) = \arg \min_{\gamma \in \mathbb{R}^p} \left\{ \frac{1}{2\delta} \|\gamma - \beta\|_2^2 + J(\gamma) \right\}, \quad \delta > 0 \quad (8)$$

to gradient based proposal steps. For loss functions whose gradient is Lipschitz continuous with constant L , such an algorithm is guaranteed to converge to the solution as long as $\delta \in (0, 2/L)$. In practice, δ is chosen as large as possible, and we are interested in finding the smallest possible Lipschitz constant L .

With known L and fixed $\delta \in (0, 2/L)$ a proximal gradient algorithm consists of the following essential computations:

1. evaluation of the gradient of the loss
2. evaluation of the proximal operator $\text{prox}_{\delta J}$
3. evaluation of the loss function and penalty function.

The computational complexity in steps 1 and 3 is dominated by matrix-vector products, (see e.g. (3) for the soft maximin problem). The complexity in step 2 is determined by J . As noted in Beck and Teboulle (2009) when J is separable (e.g. the ℓ_1 -norm) $\text{prox}_{\delta J}$ can be computed analytically or at low cost.

If L is not known (or if $\delta \geq 2/L$ for a known, but perhaps conservative, L) we cannot guarantee convergence with a fixed choice of δ , but adding a backtracking step will ensure convergence of the iterates. This extra step will increase the per-step computational complexity of the algorithm. When the gradient is not globally Lipschitz, it is no longer guaranteed that iterating steps 1-3 will yield a solution to (7) for any fixed δ . However, it is possible to show that the NPG algorithm will converge to a solution of (7) under some regularity conditions.

Algorithm 1 NPG minimizing $F = f + \lambda J$

Require: $\beta^0, L_{\max} \geq L_{\min} > 0, \tau > 1, c > 0, M \geq 0$.

- 1: **for** $k = 0$ to $K \in \mathbb{N}$ **do**
 - 2: choose $L_k \in [L_{\min}, L_{\max}]$
 - 3: solve $\beta = \text{prox}_{\lambda J/L_k}(\beta^{(k)} - \frac{1}{L_k} \nabla f(\beta^{(k)}))$
 - 4: **if** $F(\beta) \leq \max_{[k-M]_+ \leq i \leq k} F(\beta^{(i)}) - c/2 \|\beta - \beta^{(k)}\|^2$ **then**
 - 5: $\beta^{(k+1)} = \beta$
 - 6: **else**
 - 7: $L_k = \tau L_k$ and go to 3
 - 8: **end if**
 - 9: **end for**
-

We show that s_ζ does not have a Lipschitz continuous gradient in general, but convergence of the NPG algorithm can be established under general conditions on the group loss functions h_1, \dots, h_G . Furthermore, in the special case where $h_g = -\hat{V}_g$ with all groups sharing the same design we establish that s_ζ has a globally Lipschitz continuous gradient, and we find a bound on the Lipschitz constant.

The first result states that s_ζ inherits strong convexity from an individual group loss function h_g given all h_1, \dots, h_G are convex and twice continuously differentiable. The proof is given in the appendix.

Proposition 1. Assume h_1, \dots, h_G are twice continuously differentiable. Defining $w_{g,\zeta}(\beta) := e^{\zeta h_g(\beta) - \zeta s_\zeta(\beta)}$, then $\sum_g w_{g,\zeta}(\beta) = 1$ for all $\beta \in \mathbb{R}^p$ and

$$\nabla s_\zeta(\beta) = \sum_{g=1}^G w_{g,\zeta}(\beta) \nabla h_g(\beta) \quad (9)$$

$$\begin{aligned} \nabla^2 s_\zeta(\beta) &= \sum_{i=1}^G \sum_{j=i+1}^G w_{i,\zeta}(\beta) w_{j,\zeta}(\beta) (\nabla h_i(\beta) - \nabla h_j(\beta)) (\nabla h_i(\beta) - \nabla h_j(\beta))^\top \\ &\quad + \sum_{g=1}^G w_{g,\zeta}(\beta) \nabla^2 h_g(\beta). \end{aligned} \quad (10)$$

Furthermore if h_1, \dots, h_G are convex with at least one h_g strongly convex, then s_ζ and $e^{\zeta s_\zeta}$ are strongly convex.

Proposition 1 applies to the soft maximin loss with $h_g = -\hat{V}_g$. In this case $\nabla^2 h_g = 2X_g^\top X_g/n_g$, and h_g is strongly convex if and only if X_g has rank p . Proposition 1 implies that if one of the matrices X_g has rank p , l_ζ is strongly convex. However, we also see from Proposition 1 that $\nabla^2 s_\zeta(\beta)$ is not globally bounded in general even for the soft maximin loss. Consider, for instance, the case with $G = 2$ and $p = n_1 = n_2 = 2$ with

$$X_1 = \begin{pmatrix} 1 & 0 \\ 0 & 1 \end{pmatrix} \quad \text{and} \quad X_2 = \begin{pmatrix} 0 & 0 \\ \sqrt{2} & 0 \end{pmatrix}.$$

Take also $y_1 = y_2 = 0$. When $\beta_1 = \beta_2 = \kappa$ it holds that $h_1(\beta) = h_2(\beta) = \kappa^2$ and thus $w_{1,\zeta} = w_{2,\zeta} = 1/2$ for any ζ , while

$$\begin{aligned} &(\nabla h_1(\beta) - \nabla h_2(\beta)) (\nabla h_1(\beta) - \nabla h_2(\beta))^\top \\ &= \begin{pmatrix} \beta_1^2 & -\beta_1\beta_2 \\ -\beta_1\beta_2 & \beta_2^2 \end{pmatrix} = \begin{pmatrix} \kappa^2 & -\kappa^2 \\ -\kappa^2 & \kappa^2 \end{pmatrix} \end{aligned}$$

is unbounded. The following result shows, on the other hand, that for soft maximin estimation with identical X_g -matrices across the groups, ∇l_ζ is, in fact, Lipschitz continuous. The proof is in the appendix.

Corollary 1. Let $h_g = -\hat{V}_g, g \in \{1, \dots, G\}$, with identical $n \times p$ design matrix X across all G groups. Then ∇l_ζ^2 is bounded by

$$L \left(\frac{2}{n} \sum_{i=1}^G \sum_{j=i+1}^G w_{i,\zeta}(\beta) w_{j,\zeta}(\beta) \|y_i - y_j\|_2^2 + 1 \right) \leq L \left(\frac{2}{n} \sum_{i=1}^G \sum_{j=i+1}^G \|y_i - y_j\|_2^2 + 1 \right), \quad (11)$$

where $L := 2\|X^\top X\|/n$ is the Lipschitz constant of ∇h_g implying l_ζ has Lipschitz continuous gradient.

By Corollary 1 if we have identical design across groups we can obtain the soft maximin estimator by applying the fast proximal gradient algorithm from Beck and Teboulle (2009) to the optimization problem (7). Furthermore in this setting the corollary also gives an explicit upper bound on the Lipschitz constant. When L , the Lipschitz constant of the gradient of the group loss, is computable it provides a way to find an efficient step size.

Finally, in the general setup the following proposition shows that the non-monotone proximal gradient (NPG) algorithm (see Wright et al. (2009) and Chen et al. (2016)), which does not rely on a global Lipschitz property, solves the problem (7) given the assumptions in Proposition 1. The proof of the proposition is given in the appendix.

Proposition 2. *Assume h_1, \dots, h_G satisfy the assumptions in Proposition 1. Let $(\beta^{(k)})_k$ be a sequence of iterates obtained by applying the NPG algorithm to (7). Then $\beta^{(k)} \rightarrow \beta^*$ where β^* is a critical point of $s_{\zeta} + \lambda J$.*

In summary given strong convexity, e.g. satisfied in the maximin setup when one X_g has full rank, we can always solve the problem (7) using a proximal gradient based algorithm. Furthermore for soft maximin estimation with identical design across groups we can even apply a standard version of this algorithm. This is particularly convenient in the array tensor setup described next where the bound (11) is easy to compute.

3.1 Array tensor smoothing

Consider the situation where the observations in (5) are made in a d -dimensional grid G times. That is, for each $g \in \{1, \dots, G\}$ we have samples from all points in a product set

$$\mathcal{X}_1 \times \mathcal{X}_2 \times \dots \times \mathcal{X}_d \quad (12)$$

where $\mathcal{X}_j = \{x_{j,1}, \dots, x_{j,n_j}\} \subset \mathbb{R}$ with $x_{j,k_j} < x_{j,k_j+1}$ for $k_j = 1, \dots, n_j - 1$. We may organize such a sample as a d -dimensional (response) array Y_g . Preserving this array structure when formulating the smoothing model in Section 2 leads to an estimation problem with array-tensor structure. Especially, when considering the smoothing model (5) with array data the tensor structure arise if we use tensor product basis functions. Letting $n = \prod_j^d n_j$ and $p = \prod_j^d p_j$ we can use the tensor product construction to specify the multivariate basis functions appearing in (6) in terms of d univariate functions as

$$\varphi_m = \varphi_{1,m_1} \varphi_{2,m_2} \dots \varphi_{d,m_d}. \quad (13)$$

Here $\varphi_{j,m_j} : \mathbb{R} \rightarrow \mathbb{R}$ for $j = 1, \dots, d$ and $m_j = 1, \dots, p_j$ are marginal basis functions. Evaluating each of the p_j univariate functions at the n_j points in \mathcal{X}_j results in an $n_j \times p_j$ marginal design matrix $\Phi_j = (\varphi_{j,m_j}(x_{j,k_j}))_{k_j, m_j}$. It follows that the tensor (Kronecker) product of these marginal design matrices,

$$\Phi = \Phi_d \otimes \dots \otimes \Phi_2 \otimes \Phi_1, \quad (14)$$

is a design matrix for the g th group in (5).

Organizing the corresponding basis coefficients in a $p_1 \times \dots \times p_d$ array $\Theta_g = (\Theta_{j_1, \dots, j_d, g})_{j_1=1, \dots, j_d=1}^{p_1, \dots, p_d}$ and using the rotated H -transform ρ , see Currie et al. (2006), it follows that we can write the model (5) for the g th group as

$$Y_g = \rho(\Phi_d, \rho(\Phi_{d-1}, \dots, \rho(\Phi_1, \Theta_g))) + E_g \quad (15)$$

where E_g is a $n_1 \times n_2 \times \dots \times n_d$ array containing the error terms. As detailed in Currie et al. (2006), using ρ the matrix-vector products needed when evaluating the gradient and the loss in steps 1 and 3 above can be computed without having access to the (large) matrix Φ . In addition this computation is very efficient.

Furthermore because of the tensor structure in (14) the constant L from Corollary 1 is easy to compute, see (30) in Lund et al. (2017). Thus the upper bound in the corollary is computable which in turn implies that we can run the proximal gradient algorithm without performing any backtracking. Note however that the sum on the left hand side of (11) is potentially much smaller than the sum on the right since the weights are convex. Thus an efficient implementation could e.g. entail scaling down this sum and then monitor the convergence. Also note that this type of step size optimization may also be used in the NPG algorithm to enhance performance.

Following Lund et al. (2017) we have implemented both a fast proximal algorithm as well as a NPG algorithm in a way that exploits the array-tensor structure described above. These implementations are available for 1D, 2D, and 3D array data in the R package SMMA. The result is a computationally efficient numerical procedure for solving the soft maximin problem (7) with a small memory footprint.

3.2 3-dimensional signal extraction

To demonstrate soft maximin estimation in a multi-dimensional setting we simulated $G = 50$ groups of 3-dimensional signals. The signals were generated in a way similar to the 1-dimensional example from Section 2.2 and bear some resemblance to the neuronal activity imaging data. Specifically, we simulated signals with the common signal $f(x, y, t) = \varphi_{12.5,4}(x)\varphi_{12.5,4}(y)\varphi_{50,25}(t)$ (φ_{μ, σ^2} is the density for the $\mathcal{N}(\mu, \sigma^2)$ distribution) that we want to extract. This signal was superimposed with random cyclic components and white noise. The 4-dimensional raw data array was generated as

$$Y_{i,j,k,g} = f(x_i, y_j, t_k) + 5 \sum_{j \in J_g} \varphi_j(x_i + p_g)\varphi_j(y_i + p_g)\varphi_j(t_k + p_g) + \epsilon_{i,j,k,g}$$

with all components and quantities but f as in Section 2.2, and with $x_i = 1, 2, \dots, 25$, $y_i = 1, 2, \dots, 25$ and $t_i = 1, 2, \dots, 101$. We note that compared to

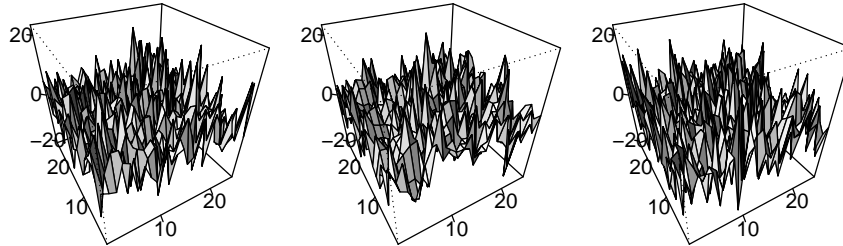


Figure 2: Three examples of 3D simulated signals at time $t_k = 50$. The common signal is not visible.

the 1-dimensional example the common signal is spatially as well as temporally localized.

Figure 2 shows the simulated signals for three different groups at time $t_k = 50$ where f attains its maximum. The common signal is visually undetectable from the individual signals. However, systematic fluctuations caused by the spatial part of the periodic random signal are visible and can be seen to differ between groups.

To extract the common signal we used the array-tensor formulation from Section 3.1 of the smoothing model from Section 2.1. Using B-splines as basis functions in each dimension we obtained an array model with tensor design components Φ^x , Φ^y , and Φ^t given by the B-spline basis function evaluations. We solved the soft maximin problem (7) with ℓ_1 -norm penalty and $\zeta = 100$.

To obtain the magging estimates we also solved an ℓ_1 -norm penalized least squares estimation problem for each group using the same design components and the same sequence of 10 penalty parameters as for the soft maximin problem using the R package `glmlasso`, Lund (2018). Given the G estimates we aggregated them as described in Bühlmann and Meinshausen (2016). We note that the time to compute the soft maximin estimate was around 30 seconds while it took around 140 seconds to compute the magging estimate. For the magging estimate the bulk of the computational time was spent estimating the group parameters. Finally, we computed the mean aggregated estimate across groups as well as the mean signal.

To select the penalty parameter we performed the following variation of 10 fold cross-validation. In each fold we left out all observations in a randomly selected $5 \times 5 \times 101$ block and fitted the model on the remaining data for each of the 10 penalty values $\lambda_1, \dots, \lambda_{10}$ from the original fit. We did this 10 times and then computed the average (over folds) soft maximin loss on the held out observations for each λ_m . The result is shown in Figure 3.

Figure 4 shows the resulting estimate along the temporal dimension for one

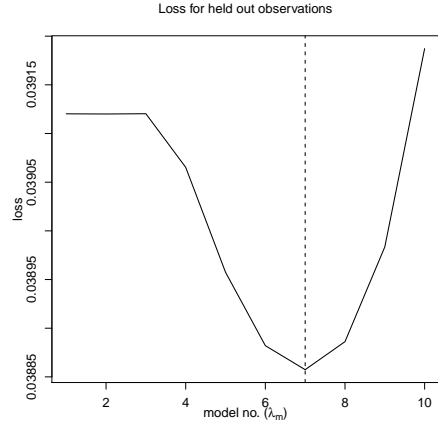


Figure 3: Generalization error for soft maximin. Dashed line is the minimum.

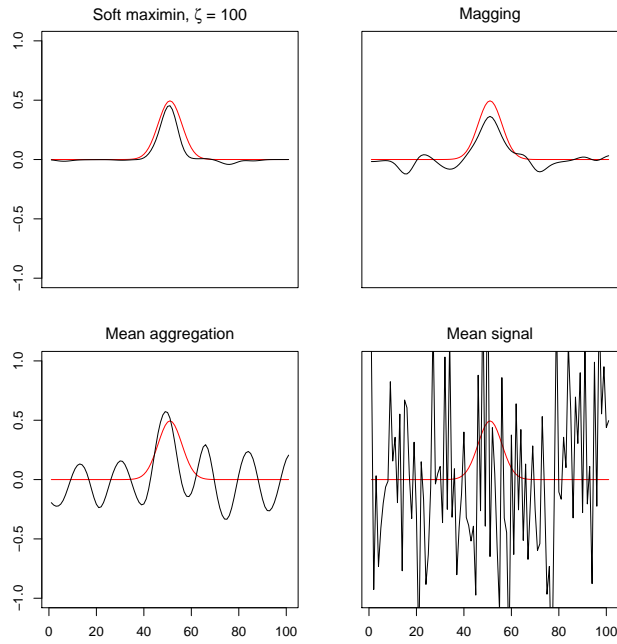


Figure 4: Bottom: Temporal plots for $(x, y) = (12, 12)$. True signal in red. Soft maximin estimate, model no. 7 and $\zeta = 100$ (top left), magging estimate (top right), mean aggregated estimate (bottom left) and mean over trials (bottom right). Soft maximin MSE is 5.5×10^{-4} and magging MSE 2.8×10^{-3} .

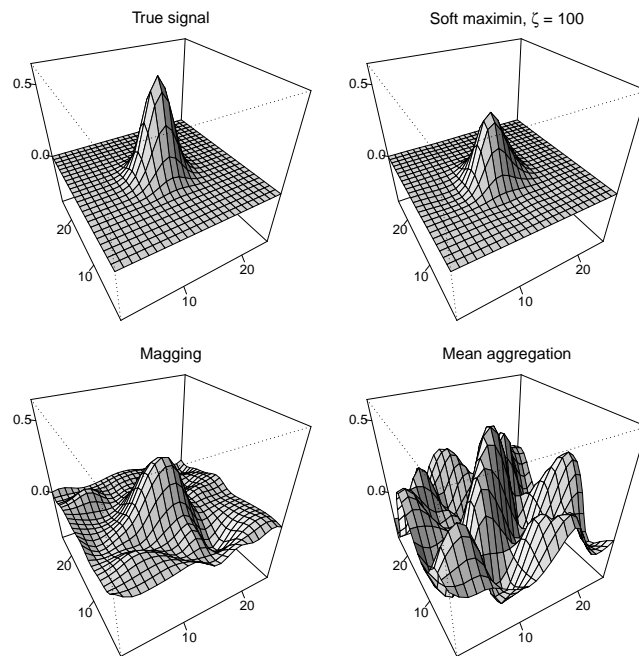


Figure 5: Spatial plots for $t_k = 50$. True signal (top left), soft maximin estimate (model no. 7), $\zeta = 100$ (top right), magging estimate (bottom left), mean aggregated estimate (bottom right).

spatial coordinate. Soft maximin (for the optimal model no. 7) with $\zeta = 100$ was able to extract the common signal quite well. The magging estimate (likewise using model no. 7 for each group) also extracted the common signal but with some additional fluctuations giving the estimate more variability. The mean aggregated estimate (model no. 7) was not able to clearly extract the common signal but rather extracted some spurious periodic fluctuations. Finally, the mean signal across the groups does not reveal the common signal at all.

Figure 5 shows the same results but plotted in the two spatial dimensions for the single time point $t_k = 50$. The figure confirms the findings from Figure 4.

4 Brain imaging data

The neuronal activity recordings were obtained using voltage-sensitive dye imaging (VSDI) in an experiment previously described in Roland et al. (2006). The experiment consisted of a total of $G = 275$ trials (groups) of recordings on 13 different ferrets. Each recording consists of a movie representing neuronal activity, which we have mapped into a 3-dimensional array for our analysis.

In short, the experimental setup was as follows. Part of the visual cortex of a live ferret was exposed and stained with a voltage-sensitive dye. Changes in neuron cell membrane potentials affect the absorption or emission fluorescence of the dye, and neuronal activity can be recorded indirectly in terms of emitted fluorescent light. The recording used 464 channels organized in a two-dimensional (hexagonal) array producing images of *in vivo* neuronal activity. In each trial a visual stimulus was presented to the live ferret (a white square on a grey screen) for 250 ms. Over the course of the trial images were recorded every 0.6136 ms producing a movie of neuronal activity. For the purpose of our analysis, the 464 channels were mapped to a 25×25 array yielding an image with 625 pixels. Note that data for 161 pixels are then unobserved.

Several sources of heterogeneity are potentially present in the data. We list some here.

1. The heart beat affects the light emission by expanding the blood vessels in the brain, creating a cyclic heart rate dependent artefact. A changing heart rate over trials for one animal (fatigue) as well as differences in heart rate between animals will cause heterogeneity in the data.
2. Spatial inhomogeneities can arise due to differences in the cytoarchitectural borders between the animals causing misalignment problems.
3. The VSDI technique is very sensitive, see Grinvald and Bonhoeffer (2002). Even small changes in the experimental surroundings could affect the recordings and create heterogeneity.
4. There are differences between animals in how they respond to the visual stimulus.

To alleviate the heart rate artefact, the raw VSDI recordings were preprocessed as follows. Two consecutive recordings were actually made in each trial; one with a visual stimulus and one without stimulus. These recordings were temporally aligned using electrocardiography (ECG) data, and the difference between these two aligned recordings was computed and normalized with the pixel-specific pre-stimulus standard deviation. We refer to the result as the preprocessed recordings.

Figures 6 and 7 show examples of the raw recordings as well as the preprocessed recordings for three trials. Figure 6 shows the recordings in the temporal dimension for one pixel, while Figure 7 shows the recordings in the spatial dimension around the time of an expected maximal stimulus response. Following the onset of the visual stimulus (200 ms), the recordings are expected to show the result of a depolarization of neuron cells in the visual cortex, but we do not observe a clear stimulus response for all trials. While trial 40 shows clear evidence of depolarization, the other two trials do not. Visual inspection of Figure 6 also indicates the presence of systematic noise components, that is, artefacts as described in 1) in the list above, which are most pronounced for the raw recordings.

4.1 Model fitting

For both the raw and the preprocessed recordings we extracted a common signal across trials and animals by soft maximin estimation, which we compared to mean aggregation and magging of the OLS estimates. The data consists of 275 spatio-temporal recordings each with dimensions $25 \times 25 \times 977$, that is, 625 pixels recorded over 977 time points (600 ms). We used 10 B-splines in each spatial dimension and 196 B-splines in the temporal dimension to obtain a linear array model with tensor design components Φ^x , Φ^y , and Φ^t , as described in Section 3.1, given by the B-splines evaluated over the marginal domains. The resulting model has a total of $p = 19,600$ parameters.

The soft maximin problem (7) was solved for the entire data set using the ℓ_1 -penalty for 10 values of the penalty parameter λ and $\zeta = 2$ and $\zeta = 100$, while the magging estimate was obtained by computing the OLS estimate for each trial and then applying maximin aggregation. The mean aggregated fit was computed likewise. All estimates were computed for the raw as well as for the preprocessed recordings. We note that to compute the 10 soft maximin estimates it took around 60 seconds (110 seconds) for the raw (preprocessed) recordings. The computation of one magging estimate took around 100 seconds (110 seconds) for the raw (preprocessed) recordings. All computations were carried out on a Macbook Pro with a 2.8 GHz Intel core i7 processor and 16 GB of 1600 MHz DDR3 memory. Movies of the estimates for both raw and preprocessed recordings are available as supplementary material.

To choose the optimal penalty parameter we randomly excluded two $5 \times 5 \times 977$ blocks of data for all trials and fitted the model on the remaining data using the 10 penalty values $\lambda_1, \dots, \lambda_{10}$ from the original fit. The soft maximin loss was then computed on the excluded data blocks for each value of the

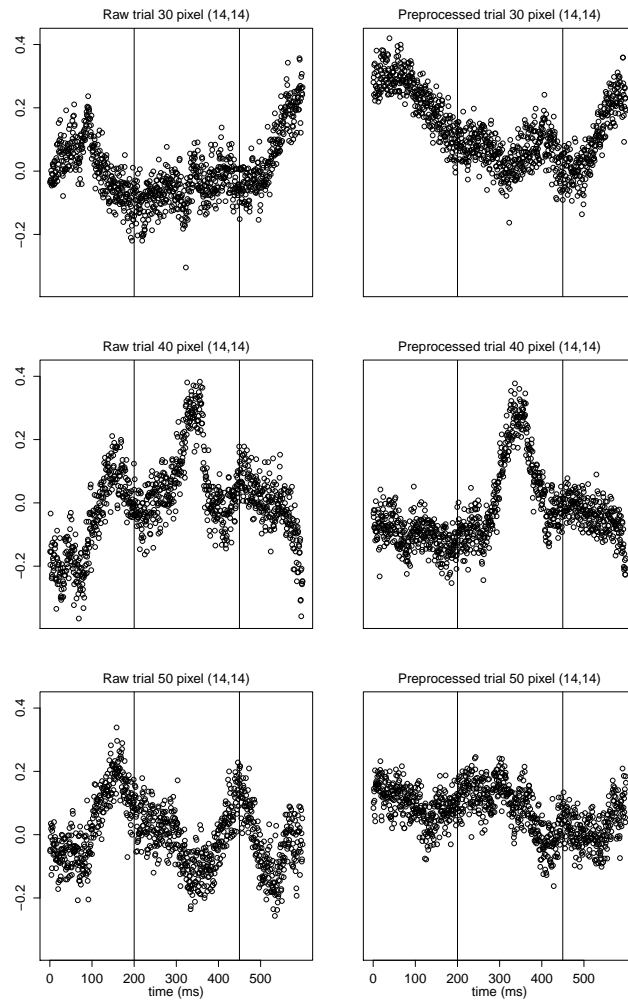
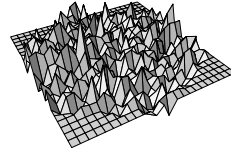
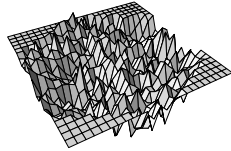


Figure 6: Temporal evolution in the raw (left) and preprocessed (right) VSDI recording from pixel (14,14) for trials 30 (top), 40 (middle), and 50 (bottom). Vertical lines indicate stimulus start (200 ms) and stop (450 ms).

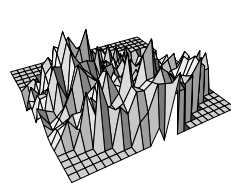
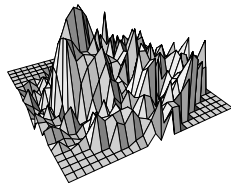
Raw trial 30 after 300 ms

Preprocessed trial 30 after 300 ms



Raw trial 40 after 300 ms

Preprocessed trial 40 after 300 ms



Raw trial 50 after 300 ms

Preprocessed trial 50 after 300 ms

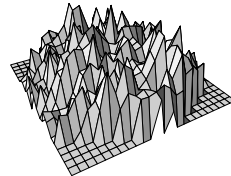
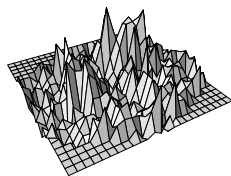


Figure 7: The raw recordings (left) and the preprocessed recordings (right) for three different trials around the time of an expected maximal response. Trial 40 shows the strongest response to the stimulus whereas the other two trials show less response. The response is strongest in the preprocessed data.

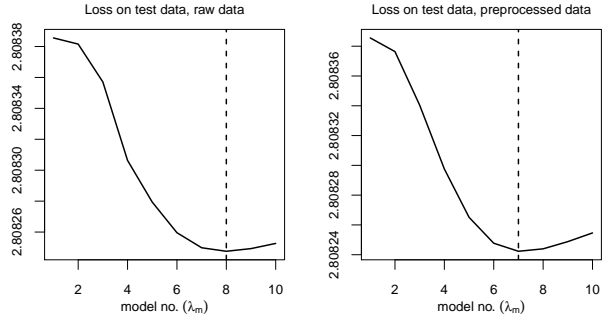


Figure 8: Validation estimates for the soft maximin loss with $\zeta = 2$ (applied to the raw recordings (left) and preprocessed recordings (right)). Dashed lines indicate minimum average soft maximin loss on held-out observations.

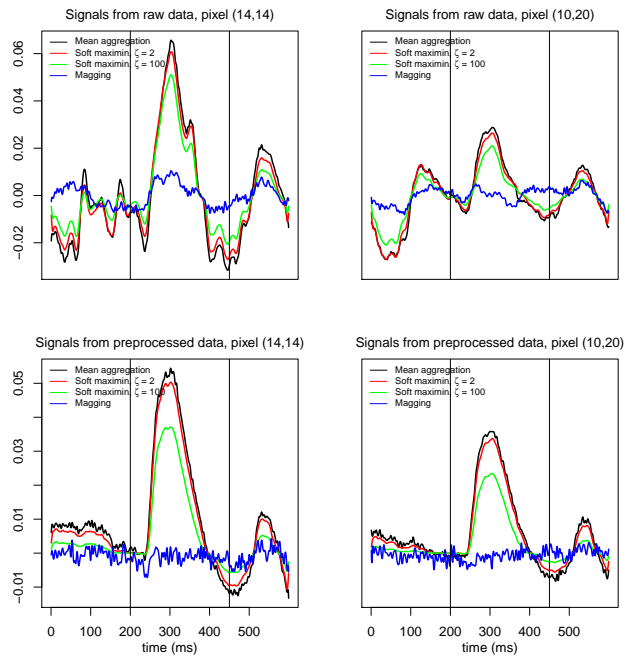


Figure 9: Temporal estimates for two different pixels using mean aggregation (black), soft maximin for $\zeta = 2$ (red) and $\zeta = 100$ (green), and magging (blue). For the raw recordings (top) model 8 was selected in the validation step while for the preprocessed recordings (bottom) model 7 was selected. Vertical lines indicate stimulus start and stop.

penalty parameter. The entire procedure was repeated ten times, the average loss was computed, and the penalty parameter with the minimal average loss was selected. This resulted in model number 8 for the raw recordings and model number 7 for the preprocessed recordings, see Figure 8.

Figure 9 shows the soft maximin (model 8), mean aggregation and magging estimates in the temporal dimension for pixels (14, 14) and (10, 20).

Mean aggregation and soft maximin estimation extract fairly clear signals both for the raw and preprocessed recordings, and a clear on-signal (stimulus start) and off-signal (stimulus stop) for these pixels are picked up. Soft maximin gives some smoothing but also some shrinkage compared to mean aggregation. The magging estimator extracts mostly noise for the preprocessed data, while showing a weak signal for pixel (14, 14) for the raw recordings.

We note that for the raw recordings both estimates display some variation, which is possibly periodic. In particular, for pixel (10, 20) a notable polarization before the stimulus is presented is picked up. This could be due to the heart rate artefact.

Figures 10 and 11 show soft maximin, mean aggregation and magging estimates in the spatial dimensions for six different time points. For the preprocessed recordings, mean aggregation resulted in a signal with a clear stimulus response. Soft maximin provided a similar result with a greater spatial localization but also shrinkage of the signal magnitude. The more compactly supported spatial area identified by soft maximin corresponds to the representation on the image of the center of field of view. For the raw data, mean aggregation resulted in some spurious spatial fluctuations that were smoothed away by soft maximin. Magging was not able to extract a signal from neither the raw nor the preprocessed recordings.

5 Discussion

The maximin estimator with the ℓ_1 -penalty, as defined in Meinshausen and Bühlmann (2015), solves the minimization problem

$$\min_{\beta} \max_g \{-\hat{V}_g(\beta)\} + \lambda \|\beta\|_1. \quad (16)$$

Though the objective function is convex, it is nondifferentiable as well as non-separable, and contrary to the claim in Section 4 of Meinshausen and Bühlmann (2015), coordinate descent will not always solve (16).

Two approximate approaches for solving (16) were suggested in Meinshausen and Bühlmann (2015), the first consisting of a proposed smooth approximation of the term $\max_g \{-\hat{V}_g(\beta)\}$. However, we did not find this approximation to work in practice, and we developed the soft maximin loss as a better alternative. We note that the solution path of (16) is piecewise linear in λ , and it may thus be computed using a method like LARS, see Roll (2008). A LARS-type algorithm or a coordinate descent algorithm of a smooth majorant, such as the soft maximin loss, was also proposed to us by Meinshausen (personal

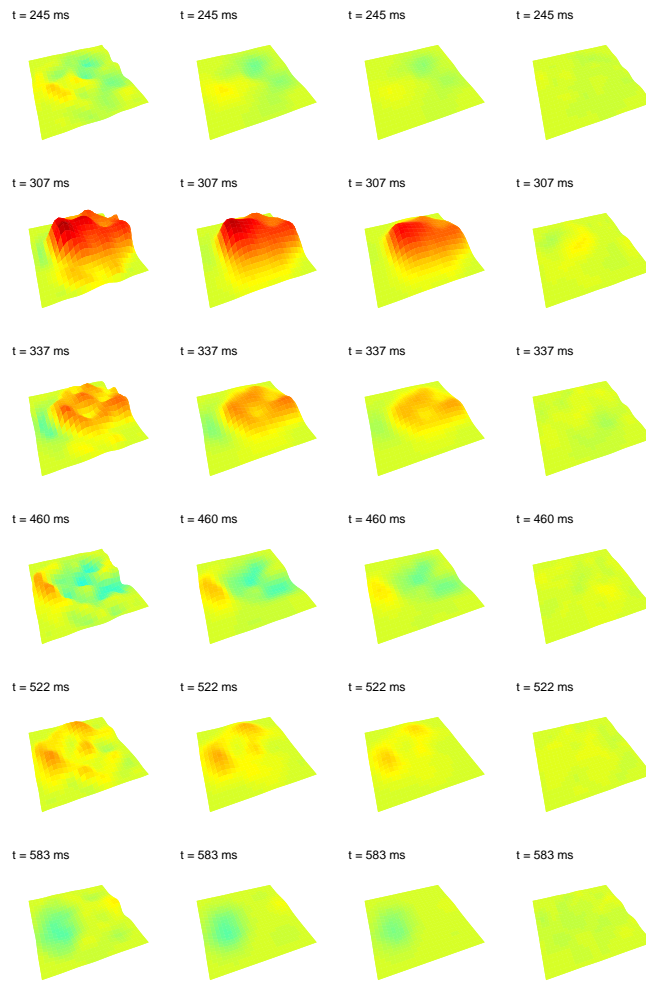


Figure 10: Spatial estimates at six different time points using the raw recordings and mean aggregation (col. 1), soft maximin for model no. 8 and $\zeta = 2$ (col. 2) and $\zeta = 100$ (col. 3), and magging (col. 4).

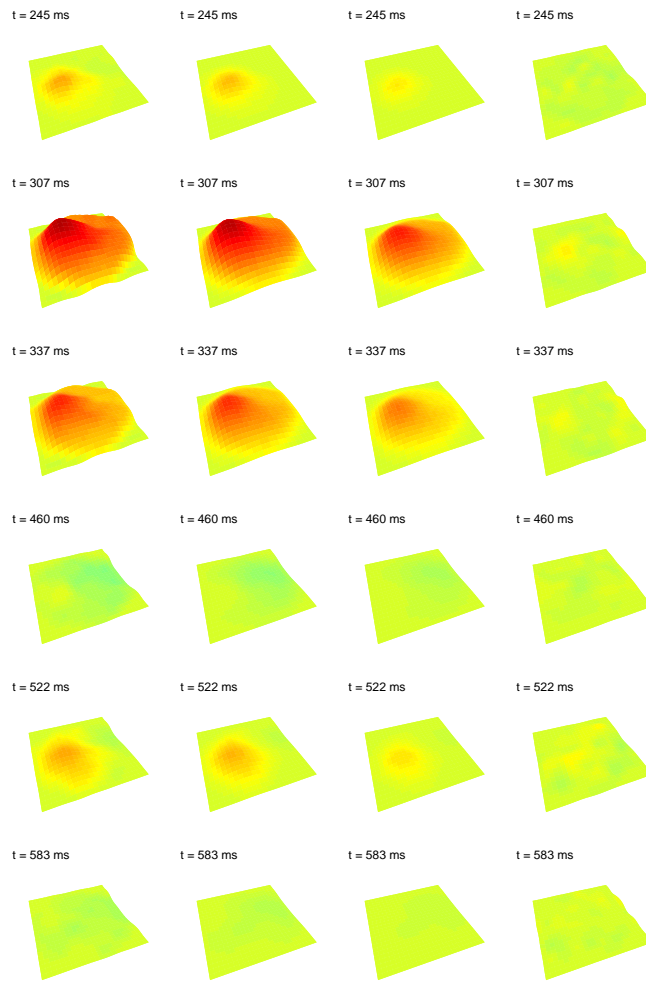


Figure 11: Spatial estimates at six different time points for the preprocessed recordings using mean aggregation (col. 1), soft maximin (model no. 8) with $\zeta = 2$ (col. 2), with $\zeta = 100$ (col. 3), and magging (col. 4).

communication) as better alternatives to those suggested in Meinshausen and Bühlmann (2015). In our experience, the LARS-type algorithm scales poorly with the size of the problem, and neither LARS nor coordinate descent can exploit the array-tensor structure.

Magging, as proposed in Bühlmann and Meinshausen (2016) as yet another alternative to (16) for estimation of maximin effects, is computationally straightforward and easy to parallelize, but as we demonstrated not necessarily computationally faster than using soft maximin aggregation.

From the definition of the soft maximin loss the intention of ζ is to control the tradeoff in the estimation between groups with large explained variance and groups with small explained variance. The gradient representation (9) shows explicitly how this tradeoff works in the NPG algorithm: the gradient of the soft maximin loss is a convex combination of the gradients of the groupwise squared error loss functions with weights controlled by ζ . The largest weights are on those groups with the smallest explained variances and as $\zeta \rightarrow \infty$ the weights concentrate on the groups with minimal explained variance. Thus our proposed algorithm and implementation in the R package *SMMA* provides a means for approximately minimizing (16) and is as such an alternative to magging as an estimator of the maximin effect. More importantly, by the introduction of the tuning parameter ζ in the soft maximin loss we not only achieved an approximate solution of (16) but an interpolation between max aggregation and mean aggregation across groups.

We have demonstrated via simulations and the application to VSDI recordings how soft maximin is able to extract a signal in the context of multivariate array data and how the choice of the tuning parameter ζ affects the extracted signal. The simulations showed that magging as well as soft maximin estimation can extract a signal even in the presence of large heterogeneous noise components, but for the VSDI recordings, magging was not successful. We expect that soft maximin aggregation will be practically useful in a number of different contexts as a way of aggregating explained variances across groups. In particular because it down weights groups with a large explained variance that might simply be outliers, while it does not go to the extreme of the maximin effect, that can kill the signal completely as in the example of the VSDI recordings.

A Proofs

We first need the following technical lemma.

Lemma 1. *Assume $\sum_i w_i = 1$ and $h_i \in \mathbb{R}^p$, $i \in \{1, \dots, G\}$, $G \in \mathbb{N}$. Then*

$$\sum_i w_i h_i \left(h_i^\top - \sum_j w_j h_j^\top \right) = \sum_i \sum_{j>i} w_i w_j (h_i - h_j)(h_i - h_j)^\top.$$

Proof. First note that since $1 - w_i = \sum_{j \neq i} w_j$

$$\begin{aligned} \sum_i w_i h_i \left(h_i^\top - \sum_j w_j h_j^\top \right) &= \sum_i w_i h_i \left((1 - w_i) h_i^\top - \sum_{j \neq i} w_j h_j^\top \right) \\ &= \sum_i \sum_{j \neq i} w_i w_j h_i (h_i - h_j)^\top. \end{aligned}$$

Letting $a_{i,j} = w_i w_j h_i (h_i - h_j)^\top$ we find that

$$\begin{aligned} \sum_i \sum_{j \neq i} a_{i,j} &= \sum_i \sum_{j > i} a_{i,j} + \sum_i \sum_{i > j} a_{i,j} \\ &= \sum_i \sum_{j > i} a_{i,j} + \sum_j \sum_{i > j} a_{i,j} \quad (\text{interchange summation order}) \\ &= \sum_i \sum_{j > i} a_{i,j} + \sum_i \sum_{j > i} a_{j,i} \quad (\text{relabel summation indices}) \\ &= \sum_i \sum_{j > i} w_i w_j (h_i - h_j) (h_i - h_j)^\top, \end{aligned}$$

where we used that $a_{j,i} = -w_i w_j h_j (h_i - h_j)^\top$. \square

Proof of Proposition 1. First it is straightforward to compute the gradient of the loss

$$\begin{aligned} \nabla s_\zeta(\beta) &= \frac{\sum_{g=1}^G e^{\zeta h_g(\beta)} \nabla \zeta h_g(\beta)}{\zeta \sum_{g=1}^G e^{\zeta h_g(\beta)}} \\ &= e^{-\log(\sum_{g=1}^G e^{\zeta h_g(\beta)})} \sum_{g=1}^G e^{\zeta h_g(\beta)} \nabla h_g(\beta) \\ &= \sum_{g=1}^G w_{g,\zeta}(\beta) \nabla h_g(\beta). \end{aligned} \tag{17}$$

From this we note that the weights

$$w_{g,\zeta}(\beta) = \frac{e^{\zeta h_g(\beta)}}{\sum_{i=1}^G e^{\zeta h_i(\beta)}} \geq 0 \tag{18}$$

satisfy $\sum_g w_{g,\zeta}(\beta) = 1$ for any β .

Differentiating (17) again gives us

$$\nabla^2 s_\zeta(\beta) = \sum_{i=1}^G \nabla h_i(\beta) \nabla w_{i,\zeta}(\beta)^\top + \sum_{g=1}^G w_{g,\zeta}(\beta) \nabla^2 h_g(\beta).$$

Using the definition of $w_{i,\zeta}$ and (18) the first term is equal to

$$\begin{aligned} & \sum_i w_{i,\zeta}(\beta) \nabla h_i(\beta) \left(\nabla h_i(\beta)^\top - \sum_j w_{j,\zeta}(\beta) \nabla h_j(\beta)^\top \right) \\ &= \sum_i \sum_{j>i} w_{i,\zeta}(\beta) w_{j,\zeta}(\beta) (\nabla h_i(\beta) - \nabla h_j(\beta)) (\nabla h_i(\beta) - \nabla h_j(\beta))^\top \end{aligned}$$

where the equality follows from Lemma 1.

For a twice continuously differentiable function f it holds that f is strongly convex with parameter ν if and only if $\nabla^2 f - \nu I$ is positive semi definite. Assuming all h_i are convex and at least one is ν -strongly convex it follows directly from (10) that s_ζ is also ν -strongly convex.

Finally, the Hessian of $e^{s_\zeta(\beta)}$ is

$$\nabla^2 e^{s_\zeta(\beta)} = \nabla^2 s_\zeta(\beta) e^{s_\zeta(\beta)} + \nabla_{\beta} s_\zeta(\beta) \nabla_{\beta} s_\zeta(\beta)^\top e^{s_\zeta(\beta)}$$

where $\nabla_{\beta} s_\zeta(\beta) \nabla_{\beta} s_\zeta(\beta)^\top e^{s_\zeta(\beta)}$ is positive semi-definite for all β . Letting $m = \min_{\beta} s_\zeta(\beta) \in \mathbb{R}$, we have $e^{s_\zeta(\beta)} \geq e^m > 0$ for all β and must have $\nabla^2 e^{s_\zeta(\beta)} - \tilde{\nu} I$ is positive semi definite for some $\tilde{\nu} > 0$, showing that e^{s_ζ} is strongly convex. \square

Proof of Corollary 1. Note that $\nabla h_g(\beta) = 2X^\top(y_g - X\beta)/n$, which is Lipschitz continuous with constant $L := 2\|X^\top X\|/n$. Here $\|\cdot\|$ denotes the sub-multiplicative matrix norm induced by the 2-norm. Observe also that $\nabla h_i(\beta) - \nabla h_j(\beta) = 2X^\top(y_i - y_j)/n$. Then from Proposition 1 it follows that

$$\begin{aligned} \|\nabla^2 s_\zeta(\beta)\| &\leq \sum_i \sum_{j>i} w_{i,\zeta}(\beta) w_{j,\zeta}(\beta) \|(\nabla h_i(\beta) - \nabla h_j(\beta)) (\nabla h_i(\beta) - \nabla h_j(\beta))^\top\| \\ &\quad + \sum_g w_{g,\zeta}(\beta) \|\nabla^2 h_g(\beta)\| \\ &= \frac{4}{n^2} \sum_i \sum_{j>i} w_{i,\zeta}(\beta) w_{j,\zeta}(\beta) \|X^\top(y_i - y_j)(y_i - y_j)^\top X\| + L \\ &\leq L \left(\frac{2}{n} \sum_i \sum_{j>i} w_{i,\zeta}(\beta) w_{j,\zeta}(\beta) \|y_i - y_j\|_2^2 + 1 \right) \\ &\leq L \left(\frac{2}{n} \sum_i \sum_{j>i} \|y_i - y_j\|_2^2 + 1 \right) \end{aligned} \tag{19}$$

by using the properties of the matrix norm. By the mean value theorem it follows that ∇l_ζ is Lipschitz continuous with a constant bounded by (19). \square

Proof of Proposition 2. If we can show that Assumption A.1 from Chen et al. (2016) holds for the soft maximin problem (7) we can use Theorem A.1 in Chen et al. (2016) (or Lemma 4 in Wright et al. (2009)) to show that the sequence has an accumulation point. Theorem 1 in Wright et al. (2009) then establishes this accumulation point as a critical point for $F_\zeta = s_\zeta + \lambda J$.

Let $\Delta > 0, \beta_0 \in \mathbb{R}^p$, and define the set

$$A_0 = \{\beta : F_{\zeta}(\beta) \leq F_{\zeta}(\beta_0)\}$$

$$A_{0,\Delta} = \{\beta : \|\beta - \beta'\| \leq \Delta, \beta' \in A_0\}.$$

A.1(i): s_{ζ} is ν -strongly convex by Proposition 1 and since J is assumed convex it follows that F_{ζ} is strongly convex. So A_0 is compact hence $A_{0,\Delta}$ is compact as a closed neighbourhood of A_0 . As s_{ζ} is C^{∞} everywhere, ∇s_{ζ} is Lipschitz on $A_{0,\Delta}$.

A.1(ii): Is satisfied by assumptions on J .

A.1(iii): Clearly $F_{\zeta} \geq 0$. Furthermore F_{ζ} is continuous hence uniformly continuous on the compact set A_0 .

A.1(iv) $\sup_{\beta \in A_0} \|\nabla s_{\zeta}\| < \infty$ as A_0 is compact and ∇s_{ζ} is continuous. Moreover, $\sup_{\beta \in A_0} \|J\| < \infty$ as A_0 is compact and J is continuous. Finally, also $\inf J = 0$. \square

References

- Beck, A. and M. Teboulle (2009). A fast iterative shrinkage-thresholding algorithm for linear inverse problems. *SIAM Journal on Imaging Sciences* 2(1), 183–202.
- Bühlmann, P. and N. Meinshausen (2016). Magging: maximin aggregation for inhomogeneous large-scale data. *Proceedings of the IEEE* 104(1), 126–135.
- Chen, X., Z. Lu, and T. K. Pong (2016). Penalty methods for a class of non-lipschitz optimization problems. *SIAM Journal on Optimization* 26(3), 1465–1492.
- Currie, I. D., M. Durban, and P. H. Eilers (2006). Generalized linear array models with applications to multidimensional smoothing. *Journal of the Royal Statistical Society: Series B (Statistical Methodology)* 68(2), 259–280.
- Grinvald, A. and T. Bonhoeffer (2002). Optical imaging of electrical activity based on intrinsic signals and on voltage sensitive dyes: The methodology.
- Lund, A. (2017). *SMMA: Soft Maximin Estimation for Large Scale Array-Tensor Models*. R package version 1.0.1.
- Lund, A. (2018). *glamlasso: Penalization in Large Scale Generalized Linear Array Models*. R package version 3.0.
- Lund, A., M. Vincent, and N. R. Hansen (2017). Penalized estimation in large-scale generalized linear array models. *Journal of Computational and Graphical Statistics* 26(3), 709–724.
- Meinshausen, N. and P. Bühlmann (2015). Maximin effects in inhomogeneous large-scale data. *The Annals of Statistics* 43(4), 1801–1830.

- Roland, P. E., A. Hanazawa, C. Undeman, D. Eriksson, T. Tompa, H. Nakamura, S. Valentiniene, and B. Ahmed (2006). Cortical feedback depolarization waves: A mechanism of top-down influence on early visual areas. *Proceedings of the National Academy of Sciences* 103(33), 12586–12591.
- Roll, J. (2008). Piecewise linear solution paths with application to direct weight optimization. *Automatica* 44(11), 2732–2737.
- Scheipl, F., A.-M. Staicu, and S. Greven (2015). Functional additive mixed models. *Journal of Computational and Graphical Statistics* 24(2), 477–501.
- Staicu, A.-M., C. M. Crainiceanu, and R. J. Carroll (2010). Fast methods for spatially correlated multilevel functional data. *Biostatistics* 11(2), 177–194.
- Tseng, P. and S. Yun (2009). A coordinate gradient descent method for nonsmooth separable minimization. *Mathematical Programming* 117(1-2), 387–423.
- Wang, J.-L., J.-M. Chiou, and H.-G. Müller (2016). Functional data analysis. *Annual Review of Statistics and Its Application* 3(1), 257–295.
- Wright, S. J., R. D. Nowak, and M. A. Figueiredo (2009). Sparse reconstruction by separable approximation. *IEEE Transactions on Signal Processing* 57(7), 2479–2493.